

# Structure and photoinduced volume changes of obliquely deposited amorphous selenium

R. Lukács,<sup>1,a)</sup> J. Hegedüs,<sup>2</sup> and S. Kugler<sup>1</sup>

<sup>1</sup>*Department of Theoretical Physics, Budapest University of Technology and Economics, H-1521 Budapest, Hungary*

<sup>2</sup>*Department of Chemistry, University of Cambridge, Lensfield Road, Cambridge CB2 1EW, United Kingdom*

(Received 6 August 2008; accepted 6 October 2008; published online 18 November 2008)

Atomic scale computer simulations on structures and photoinduced volume changes of flatly and obliquely deposited amorphous selenium (*a*-Se) films have been carried out in order to understand how the properties of chalcogenide glasses are influenced by their preparation method. Obliquely deposited *a*-Se thin films contain more coordination defects and larger voids than the flatly deposited ones. To model the photoinduced volume changes the electron excitation and hole creation were treated independently within the framework of tight-binding formalism. Covalent and interchain bond breakings and formations were found. The obliquely deposited samples containing voids showed a wide spectrum of photoinduced structural changes in the microscopic level and volume changes in the macroscopic level. © 2008 American Institute of Physics.

[DOI: [10.1063/1.3021464](https://doi.org/10.1063/1.3021464)]

## I. INTRODUCTION

Chalcogenide glasses show a variety of photoinduced effects during band-gap illumination, such as photoinduced volume change (expansion or contraction), photodarkening, photobleaching, photodensification, etc.<sup>1</sup> It is important to learn their properties because they have technological applications, e.g., optical disk, electronic nonvolatile memory technology (phase-change random-access memory, etc.<sup>2</sup> Several experiments have been performed since the discovery of photoinduced effects in order to understand their kinetics. One of the first steps was the mapping of the structure. At the end of the 1970s photoinduced effects were studied by Singh *et al.*<sup>3</sup> They have concluded that these photoinduced effects in chalcogenide films could be enhanced by oblique deposition. In amorphous GeSe films a correlation was observed between the anomalously large photocontraction and the angle of deposition. Columnar structures were found in these films.

In obliquely deposited amorphous GeSe<sub>3</sub> films density decreased when the angle of the evaporant beam increased, as was reported by Rayment and Elliott.<sup>4</sup> Columnar structures of these materials were also found. The illumination with band-gap light caused photodensification.<sup>4</sup> The columnar structure was observed in obliquely deposited *a*-GeS<sub>2</sub>,<sup>5</sup> too. Decrease in the refractive index and microhardness versus angle of incidence has been reported. These are evidences of the increasing free volume with the increase in obliqueness.<sup>5</sup> Photoinduced changes in optical properties of obliquely deposited *a*-As<sub>2</sub>S<sub>3</sub> thin films have been studied by Dikova *et al.*<sup>6</sup> They found that the increase in the refractive index and absorption coefficient is higher in the case of obliquely deposited films. Recently giant photoinduced expansion was investigated by Tanaka *et al.*<sup>7</sup>

A comparison between obliquely deposited As-based and Ge-based chalcogenide films was performed by Kuzukawa's<sup>8</sup> group. Photodarkening and photoexpansion of As-based chalcogenides and photobleaching and photocontraction in Ge-based chalcogenides were measured.<sup>8</sup> From these experiments it can be concluded that obliquely deposited chalcogenides show more enhanced photoinduced changes. This could be a consequence of free volume and thus of a more porous structure.

Photoinduced volume expansion in quenched amorphous selenium using tight-binding molecular dynamics (TBMD) computer simulations has been investigated by Hegedüs *et al.*<sup>9</sup> They found covalent bond breaking in amorphous networks caused by photoinduced excited electrons, whereas holes contributed to the formation of interchain bonds. By applying the bond breaking and interchain bond formation models, they described the time development of macroscopic volume expansion in void-free amorphous selenium. Recently, Ikeda and Shimakawa<sup>10</sup> published their experimental results on flatly and obliquely deposited *a*-As<sub>2</sub>Se<sub>3</sub>. The flatly deposited sample shows photoinduced volume expansion, while the other shrinks during the illumination, and after switching off the light its volume remains the same.

In order to understand these controversial results and the detailed kinetics of the photoinduced changes we carried out further MD simulations on *a*-Se which is the model material for the chalcogenides. Binary component glass preparation is much more difficult, because at least three different interactions have to be considered<sup>11</sup> during the model construction. As a first stage a set of MD simulations were applied to grow amorphous samples in different angles of deposition, then, the obtained structures of these samples were analyzed.<sup>12</sup> Afterwards a second set of TBMD simulations were carried out to follow up the time development of photoinduced changes in the microscopic and macroscopic levels. The structure of this paper is as follows. The simulation method

<sup>a)</sup>Electronic mail: lukacsr@maxwell.phy.bme.hu.

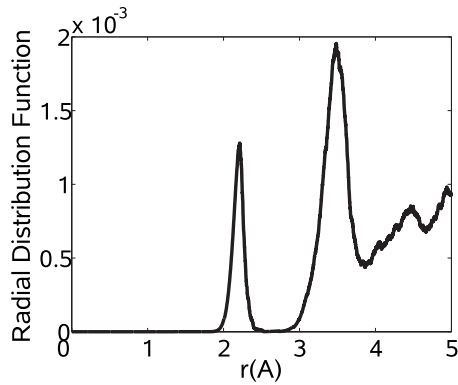


FIG. 1. RDF of an *a*-Se sample deposited by an angle of incidence equal to  $60^\circ$ .

will be presented in the second section, in third and fourth sections, the results of the analyses and some conclusions will be formulated, respectively, in the end.

## II. METHODS AND MODEL PREPARATION

A MD computer code<sup>12</sup> has been developed for the simulation of thermal evaporation growth process of flatly and obliquely deposited *a*-Se. Our purpose was to construct relatively large samples containing at least 1000 atoms. A classical empirical three-body potential was used to calculate the atomic interactions.<sup>13</sup> The simulation technique was the following. A trigonally crystalline lattice, containing 324 selenium atoms, was employed to mimic the substrate. There were 108 fixed atoms at the bottom of the substrate and the remaining 216 atoms could move with full dynamics. The simulation cell was open along the positive *z* axis and periodic boundary conditions were applied in the *x* and *y* directions. The velocity Verlet algorithm was used to follow the atomic motions. The time step was chosen to be 1 fs. Frequency of the atomic injection was  $f=1/125 \text{ fs}^{-1}$  on the average. Kinetic energy of the atoms inside the substrate was rescaled at every MD step to keep the substrate at a constant temperature. Several samples were prepared with average angles between the normal to the substrate and the direction of the randomly directed incidence atoms of  $0^\circ$ ,  $20^\circ$ ,  $45^\circ$ , and  $60^\circ$ . Temperature of the substrate was kept at 300 K, while the average bombarding energy was equal to 1 eV.

To simulate the photoinduced structural changes in these amorphous samples, a second type of MD simulation code was ran using a TB Hamiltonian.<sup>14</sup> This TBMD computer code was developed by Hegedüs *et al.*<sup>9,15</sup> It was assumed that immediately after a photon absorption the electron and the hole become separated in space on a femtosecond time

TABLE I. Densities of flatly and obliquely deposited samples.

Average angle of incidence (deg)	Density (g/cm <sup>3</sup> )
0	4.50
20	4.40
45	4.38
60	4.20

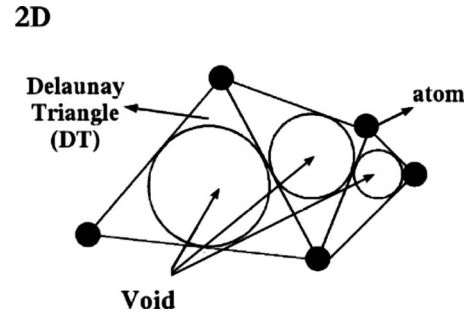


FIG. 2. Two-dimensional representation of DTs and a possible approximation of void sizes using a Delaunay-triangle intercircle.

scale.<sup>16</sup> Therefore, excited electrons and created holes can be treated independently. Two different types of simulation methods were carried out: the first one was to model the excited electron creation, an extra electron was put into the lowest unoccupied molecular orbital (LUMO), and second case, an electron in the highest occupied molecular orbital (HOMO) (hole creation) was annihilated. In this approach, excitons do not play any role during the photoinduced volume changes and the Coulomb interaction between electrons and holes are also neglected.

## III. STRUCTURE ANALYSIS

Flatly and obliquely deposited samples have been analyzed in order to obtain information about differences in their structures. Four samples have been considered prepared by incidence average angles of  $0^\circ$ ,  $20^\circ$ ,  $45^\circ$ , and  $60^\circ$ . First the radial distribution functions (RDFs) were calculated. Figure 1 shows the RDF of the sample deposited under an average angle of incidence of  $60^\circ$ . There were no relevant differences among RDFs. The first neighbor shell peak appeared at 2.35 Å, while the second neighbor one was at 3.5 Å. These values provide good agreement to x-ray diffraction measurements,<sup>17</sup> where the pair correlation functions of amorphous Se prepared by mechanical milling (MM) for 50 h and by liquid quenching (LQ) from  $600^\circ\text{C}$  have been derived. The first neighbor distance for the MM-amorphous Se was 2.36 Å and for the LQ-amorphous Se 2.37 Å. The second nearest-neighbor distances were around 3.7 Å for both samples.

Coordination number distributions of the samples were analyzed next. Most of the atoms (>90%) had a coordina-

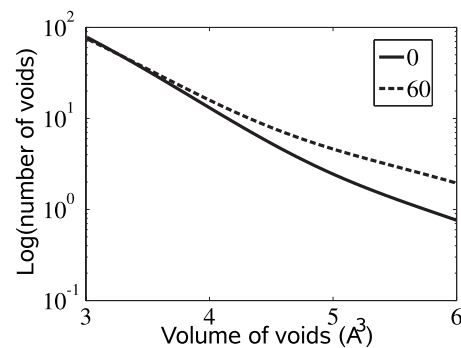


FIG. 3. Void size distributions of two different samples in the interval from 3 to  $6 \text{ \AA}^3$ .

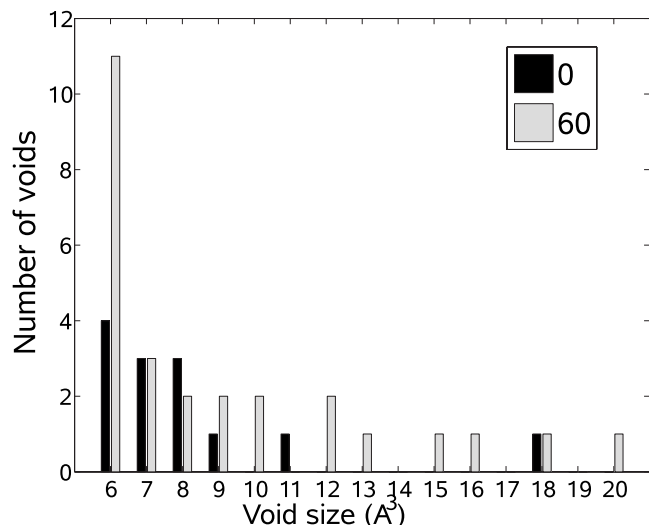


FIG. 4. Distributions of largest voids of two different samples.

tion number of two. There were atoms with a coordination number equal to three ( $\sim 9\%$ ) and very few ( $\sim 1\%$ ) with a coordination number of one. These are called coordination defects. The number of coordination defects increased by 3% if the average angle of incidence was varied from  $0^\circ$  to  $60^\circ$ .

A correlation was found between the angles of incidence and densities due to different samples, i.e., densities decreased monotonically in the function of deposition angle in the interval of  $0^\circ$ – $60^\circ$  as displayed in Table I. This fact suggests that larger voids could be found in the obliquely deposited films. In order to investigate this supposition, a void size analysis of the samples has been performed using the Voronoi–Delaunay approach.<sup>18</sup> The Voronoi diagram of a set of atoms  $i=1, N$  is a decomposition of the space into  $N$  regions (called Voronoi polyhedra) associated with each atom, i.e., every point of a Voronoi region is closer to the associated atom than to any other atom in the system. Atoms whose Voronoi polyhedra share a face are considered to be contiguous. A set of four atoms contiguous to each other forms a tetrahedron, which is called Delaunay tetrahedron (DT) in three-dimensional space (see two-dimensional representation in Fig. 2). The DT's insphere volume has been applied as a measure of void volume. Two void size distributions from 3 to 6  $\text{\AA}^3$  follow a near logarithmic distribution as shown in Fig. 3. Voids with larger volumes than 6  $\text{\AA}^3$

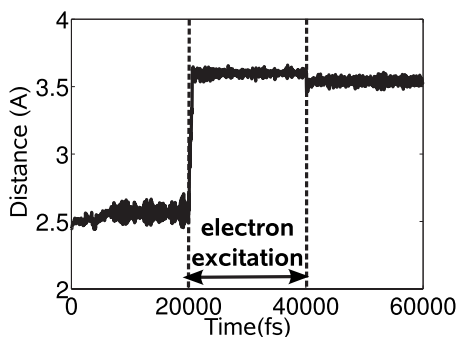


FIG. 5. Electron excitation induced irreversible covalent bond breaking.

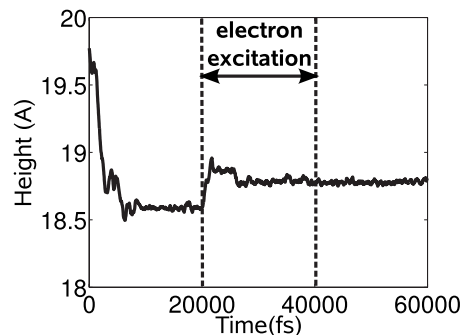


FIG. 6. A covalent bond breaking induced irreversible macroscopic photoexpansion.

presented in Fig. 4 appear mostly in the obliquely deposited samples.

#### IV. PHOTOINDUCED CHANGES

The structure of amorphous chalcogenide thin films depends strongly on the deposition angle. Our MD computer simulations confirmed that obliquely deposited films had more porous structures due to the presence of larger voids. A possible scenario for the photoinduced volume contraction of obliquely deposited films proposed by Ikeda and Shimakawa<sup>10</sup> is the following: the primary effect in these materials is the void collapsing. Bond breaking probably destroys voids, decreasing their sizes. The flatly deposited films avoid this effect because of the lack of voids.

TBMD simulations have to be carried out to gain insight in the photoinduced structural changes in amorphous selenium containing voids, i.e., the obliquely deposited *a*-Se film. Thermally well relaxed samples taken from our earlier TBMD simulation<sup>9</sup> containing 162 atoms were used as initial configurations. In the first series two overlapping ellipsoid voids<sup>4</sup> were artificially created removing Se atoms from the sample in order to make our models more realistic. Void creation procedure in this case was the following: the closest atoms to the points at one-third and two-third on the symmetry line in the  $z$  direction of the simulation cell were chosen. Centers of the ellipsoids were assigned to these atoms and 16-16 nearest-neighbor atoms to these centers were removed. In the second case several randomly distributed small spheri-

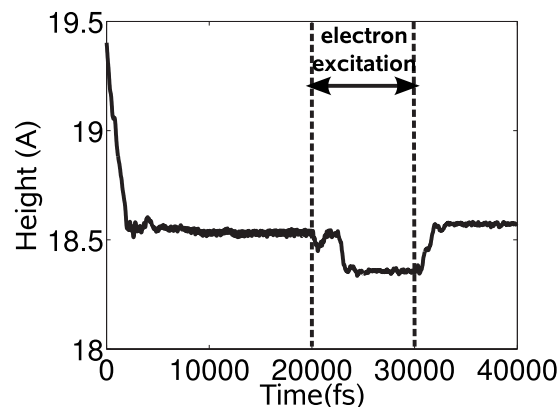


FIG. 7. Electron excitation induced reversible macroscopic photocontraction.

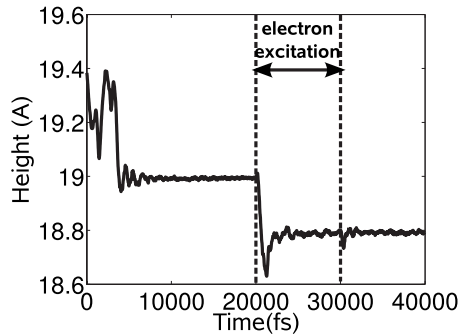


FIG. 8. Electron excitation induced irreversible macroscopic photocontraction.

cal voids with a radius of  $2.7 \text{ \AA}$  were made to mimic the obliquely deposited thin films. These new configurations (containing 100 atoms and voids) were relaxed for 20 ps or for 30 ps at 20 K temperature to stabilize the structures. After relaxation, either an extra electron (occupation of LUMO increased) or an extra hole (occupation of HOMO decreased) was put into the system. The excited state lasted for 10 ps or for 20 ps. After the excitation processes the samples were relaxed again for 10 ps or for 20 ps.

In void free *a*-Se films, Hegedüs *et al.*<sup>9</sup> found photoexpansion due to covalent bond breaking during the electron excitation process and photocontraction due to interchain bond formation in case of hole creation. Our results of the photoexcitation of oblique samples containing voids are presented below.

### A. Electron excitation

When an extraexcited electron was created photoexpansion and covalent bond breaking were observed in most of the obliquely deposited *a*-Se films, but some exotic behaviors were also found. The thickness (height) of sample in the open *z* direction was analyzed. Reversible and irreversible photoexpansions and contractions were noticed. The reversible photoexpansion was induced by a reversible covalent bond breaking as it was derived in our earlier work (See Fig. 3 in Ref. 9). An irreversible covalent bond breaking is displayed in Fig. 5. Time evolution of irreversible volume change is shown in Fig. 6. We have found that in such cases a covalent bond breaks irreversibly and causes more irreversible changes in the bonding network (all this is due to the excited electron). In some cases electron excitation can cause

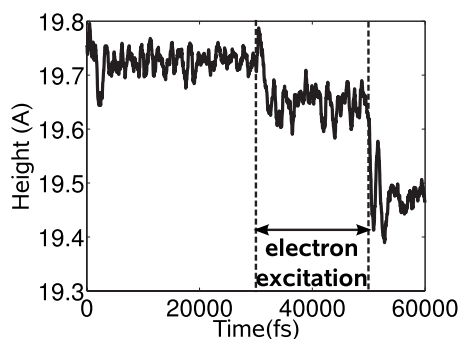


FIG. 9. Two step irreversible volume contraction.

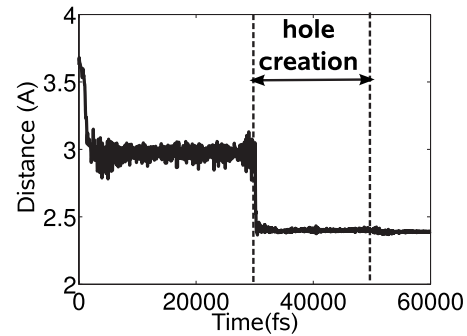


FIG. 10. Hole creation induced an irreversible covalent bond formation.

reversible photocontraction as shown in Fig. 7. The contraction must be caused by the rearrangement of the network because the photoexcitation causes reversible bond breaking (elongation) at the same time. Another exotic case found was a sample showing irreversible photocontraction induced by the electron excitation process (Fig. 8). In this case there was an irreversible covalent bond breaking and some irreversible changes in the bonding environment causing void size reduction. During the excitation process sample height decreased and further shrinkage occurred after switching off the excitation (this two step process is shown in Fig. 9). Irreversible covalent bond breaking and some irreversible structural changes on the face of the inner voids were found in this case.

### B. Hole creation

In the second set of TBMD simulations, when a hole was created, several changes due to the photoexcitation process were observed. More structural changes took place; there were chain deformations, slips, ring creations, covalent/interchain bond formations, and breakings. In most cases the height of sample decreased during hole creation and some of the samples only showed transient changes (only present during excitation) due to reversible interchain bond formations (also discussed in Fig. 4 of Ref. 9). However, irreversible covalent (not interchain!) bond formation in the void-containing network (as shown in Fig. 10) caused irreversible contraction (see Fig. 11). In Fig. 12 a composition of reversible and irreversible volume contractions can be seen where the reversible part is small, but significant chain slip was observed inside this sample. Some exotic cases were also

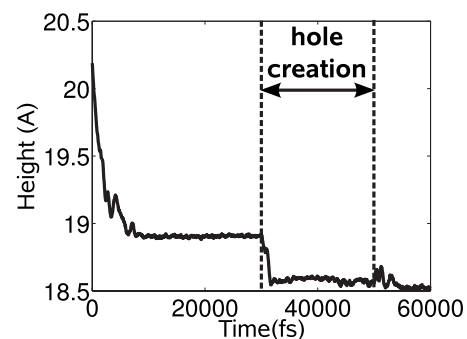


FIG. 11. Hole creation induced irreversible macroscopic photocontraction.



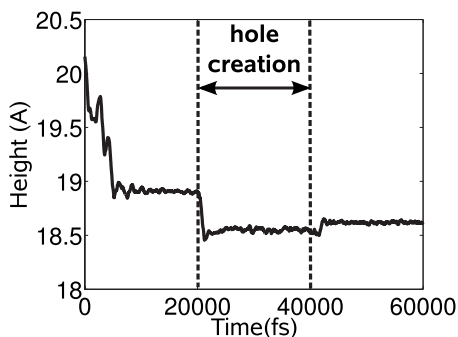


FIG. 12. Hole creation induced reversible macroscopic photocontraction.

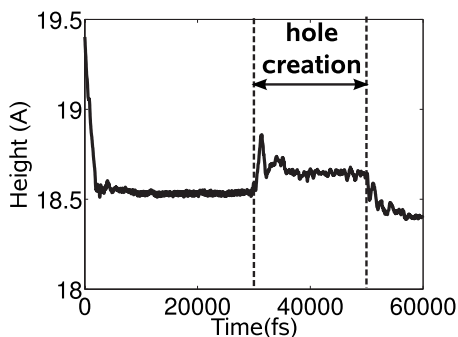


FIG. 13. Hole creation induced reversible macroscopic photoexpansion.

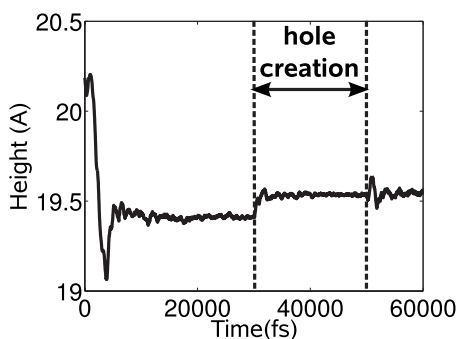


FIG. 14. Hole creation induced irreversible macroscopic photoexpansion.

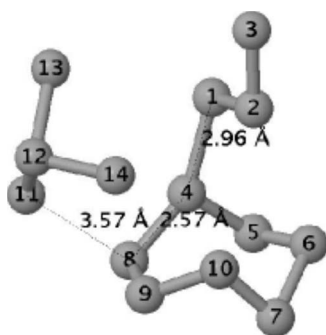
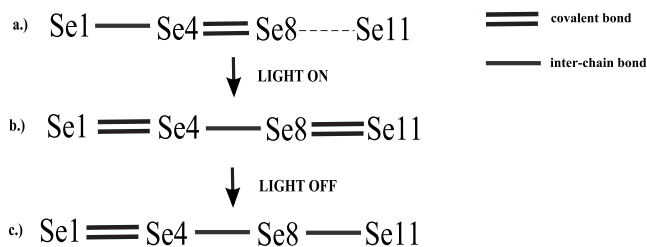


FIG. 15. Snapshot of a bonding network before the illumination process.

FIG. 16. Photoinduced covalent bond shift in an *a*-Se chain.

noticed, where the sample showed reversible (see Fig. 13) or irreversible photoexpansion as shown in Fig. 14, but nonetheless interchain bonds were formed.

### C. Photoinduced bond shift

In a Se chain a photoinduced covalent bond shift<sup>19</sup> has been observed. Figure 15 shows a snapshot of the Se chain before the illumination. Covalent bond length was considered to be between 2.2–2.6 Å while interchain bonds were between 2.8–3.4 Å. The bonding configuration before the illumination presented in Fig. 16(a) was the following: between atoms 1 and 4 an interchain bond and between atoms 4 and 8 a covalent bond were found. The hole creation process induced some changes in the bonding network. The covalent bond between Se atoms 4 and 8 got longer and became an interchain bond. Between atoms 1 and 4 and atoms 8 and 11 covalent bonds were formed [see Fig. 16(b)]. After stopping the illumination a covalent bond was formed between atoms 1 and 4. Interchain bonds between atoms 4 and 8 and between atoms 8 and 11 were also formed [Fig. 16(c)]. The covalent bond between atoms 8 and 4 shifted to atoms 4 and 1 as the result of the photoexcitation process.

In most of the samples structural changes appeared mostly in the vicinity of coordination defects but in a few samples chain slips were also found.

## V. CONCLUSIONS

MD simulations have been carried out to investigate structures and photoinduced effects of obliquely deposited *a*-Se. Increasing deposition angle leads to lower sample density. This rule can be explained by the presence of larger voids, which was confirmed by our Voronoi analysis. The TBMD simulations of photoinduced volume changes showed more varieties of microscopic and macroscopic levels than we had obtained in our earlier void free simulations.<sup>9</sup> We described in detail these complex atomic rearrangements occurring on photoexcitation in porous samples, which are reversible and irreversible photocontraction/expansion, bond breaking and formations (both inter and intrachain), chain slips, and bond shifts. Obliquely deposited chalcogenides are more sensitive to the illumination than flatly deposited samples because voids provide more degrees of freedom for atomic positions.

## ACKNOWLEDGMENTS

This work was supported by the OTKA Fund (Grant No. T048699) and the Japanese-Hungarian intergovernmental

project (Project No. JP-5/2006). We acknowledge Professor Koichi Shimakawa (Gifu University, Japan) and Krisztián Koháry (University of Exeter, U.K.) for valuable discussions. J.H. is thankful for the Marie Curie fellowship.

<sup>1</sup>*Photo-Induced Metastability in Amorphous Semiconductors*, edited by A. V. Kolobov (Wiley-VCH, Germany, 2003).

<sup>2</sup>J. Hegedüs and S. R. Elliott, *Nature Mater.* **7**, 399 (2008).

<sup>3</sup>B. Singh, S. Rajagopalan, P. K. Bhat, D. K. Pandya, and K. L. Chopra, *Solid State Commun.* **29**, 167 (1979).

<sup>4</sup>T. Rayment and S. R. Elliott, *Phys. Rev. B* **28**, 1174 (1983).

<sup>5</sup>K. Starbova, V. Mankov, J. Dikova, and N. Starbov, *Vacuum* **53**, 441 (1999).

<sup>6</sup>J. Dikova, P. Sharlandjiev, and P. Gushterova, and Tz. Babeva, *Vacuum* **69**, 395 (2002).

<sup>7</sup>Ke. Tanaka, A. Saitoh, and N. Terakado, *J. Optoelectron. Adv. Mater.* **8**, 2058 (2006).

<sup>8</sup>Y. Kuzukawa, A. Ganjoo, and K. Shimakawa, *J. Non-Cryst. Solids* **227–**

**230**, 715 (1998).

<sup>9</sup>J. Hegedüs, K. Kohary, D. G. Pettifor, K. Shimakawa, and S. Kugler, *Phys. Rev. Lett.* **95**, 206803 (2005).

<sup>10</sup>Y. Ikeda and K. Shimakawa, *J. Non-Cryst. Solids* **338–340**, 539 (2004).

<sup>11</sup>Ke. Tanaka, *Jpn. J. Appl. Phys., Part 1* **37**, 1747 (1998).

<sup>12</sup>S. Kugler, J. Hegedüs, R. Lukács, and J. Optoelectron, *J. Optoelectron. Adv. Mater.* **9**, 37 (2007).

<sup>13</sup>C. Oligschleger, R. O. Jones, S. M. Reimann, and H. R. Schober, *Phys. Rev. B* **53**, 6165 (1996).

<sup>14</sup>E. Lomba, D. Molina, and M. Alvarez, *Phys. Rev. B* **61**, 9314 (2000).

<sup>15</sup>J. Hegedüs and S. Kugler, *J. Phys.: Condens. Matter* **17**, 6459 (2005).

<sup>16</sup>D. Moses, *Phys. Rev. B* **53**, 4462 (1996).

<sup>17</sup>T. Fukunaga, M. Utsumi, H. Akatsuka, M. Misawa, and U. Mizutani, *J. Non-Cryst. Solids* **205–207**, 531 (1996).

<sup>18</sup>G. Malavasi, M. C. Menziani, A. Pedone, and U. Segre, *J. Non-Cryst. Solids* **352**, 285 (2006).

<sup>19</sup>A. V. Kolobov, H. Oyanagi, Ka. Tanaka, and Ke. Tanaka, *Phys. Rev. B* **55**, 726 (1997).